

INCLUSIVE D-MESON BRANCHING RATIOS

LEBC-EHS Collaboration

M. Aguilar-Benitez<sup>10</sup>, W.W.M. Allison<sup>12</sup>, J.L. Bailly<sup>11</sup>, W. Bartl<sup>23</sup>, M. Begalli<sup>1</sup>,  
P. Beillière<sup>6</sup>, R. Bizzarri<sup>15</sup>, H. Briand<sup>14</sup>, R. Brun<sup>5</sup>, V. Canale<sup>15</sup>, C. Caso<sup>8</sup>,  
E. Castelli<sup>22</sup>, P. Checchia<sup>13</sup>, P.V. Chliapnikov<sup>18</sup>, N. Colino<sup>10</sup>, S.J. Colwill<sup>12</sup>,  
R. Contri<sup>8</sup>, D. Crennell<sup>16</sup>, A. De Angelis<sup>13</sup>, L. de Billy<sup>14</sup>,  
C. Defoix<sup>6</sup>, R. Di Marco<sup>17</sup>, E. Di Capua<sup>15</sup>, F. Diez-Hedo<sup>10</sup>, J. Dolbeau<sup>6</sup>,  
J. Duboc<sup>14</sup>, J. Dumarchez<sup>14</sup>, M. Eriksson<sup>19</sup>, S. Falciano<sup>15</sup>, C. Fernandez<sup>5</sup>,  
C. Fisher<sup>16</sup>, Yu.V. Fisyak<sup>18</sup>, F. Fontanelli<sup>8</sup>, J. Fry<sup>9</sup>, U. Gasparini<sup>13</sup>, U. Gensch<sup>2</sup>,  
S. Gentile<sup>15</sup>, D.B. Gibaut<sup>12</sup>, A.T. Goshaw<sup>7</sup>, A. Gurtu<sup>3</sup>, R. Hamatsu<sup>21</sup>, L. Haupt<sup>19</sup>,  
S. Hellman<sup>19</sup>, V. Henri<sup>11</sup>, J.J. Hernandez<sup>5</sup>, S.O. Holmgren<sup>19</sup>, M. Houlden<sup>9</sup>,  
J. Hrubec<sup>23</sup>, P. Hughes<sup>16</sup>, D. Huss<sup>20</sup>, Y. Iga<sup>21</sup>, M. Iori<sup>5</sup>, E. Jegham<sup>20</sup>,  
K.E. Johansson<sup>19</sup>, M.I. Josa<sup>10</sup>, M. Kalelkar<sup>17</sup>, A.G. Kholodenko<sup>18</sup>,  
E.P. Kistenev<sup>18</sup>, S. Kitamura<sup>21</sup>, D. Knauss<sup>2</sup>, V.V. Kniazev<sup>18</sup>, W. Kowald<sup>7</sup>,  
D. Kuhn<sup>23</sup>, J. Laberrigue<sup>14</sup>, M. Laloum<sup>6</sup>, P. Legros<sup>11</sup>, H. Leutz<sup>5</sup>, L. Lyons<sup>12</sup>,  
M. MacDermott<sup>16</sup>, P. Mason<sup>9</sup>, M. Mazzucato<sup>13</sup>, M.E. Michalon-Mentzer<sup>20</sup>,  
A. Michalon<sup>20</sup>, T. Moa<sup>19</sup>, R. Monge<sup>8</sup>, L. Montanet<sup>5</sup>, G. Neuhofer<sup>23</sup>,  
H.K. Nguyen<sup>14</sup>, S. Nilsson<sup>19</sup>, H. Nowak<sup>2</sup>, N. Oshima<sup>21</sup>, G. Otter<sup>1</sup>, R. Ouared<sup>14</sup>,  
J. Panella Comellas<sup>12</sup>, G. Patel<sup>9</sup>, C. Patrignani<sup>15</sup>, M. Pernicka<sup>23</sup>, P. Pilette<sup>11</sup>,  
C. Pinori<sup>13</sup>, G. Piredda<sup>15</sup>, R. Plano<sup>17</sup>, A. Poppleton<sup>5</sup>, P. Poropat<sup>22</sup>,  
R. Raghavan<sup>3</sup>, S. Reucroft<sup>5</sup>, K. Roberts<sup>9</sup>, W.J. Robertson<sup>7</sup>, H. Rohringer<sup>23</sup>,  
J.M. Salicio<sup>10</sup>, R. Schulte<sup>1</sup>, B. Sellden<sup>19</sup>, M. Sessa<sup>22</sup>, S. Squarcia<sup>8</sup>, P. Stamer<sup>17</sup>,  
V.A. Stopchenko<sup>18</sup>, A. Subramanian<sup>3</sup>, K. Sudhakar<sup>3</sup>, K. Takahashi<sup>21</sup>, M.C. Touboul<sup>5</sup>,  
U. Trevisan<sup>8</sup>, C. Troncon<sup>22</sup>, T. Tsurugai<sup>21</sup>, L. Ventura<sup>13</sup>, P. Vilain<sup>4</sup>, E.V. Vlasov<sup>18</sup>,  
C. Voltolini<sup>20</sup>, B. Vonck<sup>4</sup>, W.D. Walker<sup>7</sup>, C.F. Wild<sup>7</sup>, T.P. Yiou<sup>14</sup> and G. Zumerle<sup>13</sup>

Submitted to Zeitschrift für Physik C

- 1 III. Physikalisches Inst. der Technischen Hochschule, Aachen, Germany
- 2 Institute für Hochenergiephysik der AdW der DDR, Berlin-Zeuthen, GDR
- 3 Tata Institute of Fundamental Research, Bombay, India
- 4 IIHE ULB-VUB, Brussels, Belgium
- 5 CERN, European Organization for Nuclear Research, Geneva, Switzerland
- 6 Lab. de Physique Corpusculaire, Collège de France, Paris, France
- 7 Duke University, Durham, NC, USA
- 8 Dipartimento di Fisica and INFN, Università di Genova, Genova, Italy
- 9 Phys. Dept. University of Liverpool, Liverpool, UK
- 10 CIEMAT-JEN, Madrid, Spain
- 11 Université de l'Etat à Mons, Mons, Belgium
- 12 Nuclear Physics Laboratory, University of Oxford, Oxford, UK
- 13 Dipartimento di Fisica, Università di Padova and INFN, Padova, Italy
- 14 LPNHE, Paris 6-Paris 7, Paris, France
- 15 Dipartimento di Fisica and INFN, Università of Roma, La Sapienza, Roma, Italy
- 16 Rutherford and Appleton Laboratory, Chilton, UK
- 17 Rutgers University, New Brunswick, USA
- 18 Institute for High Energy Physics, Serpukhov, USSR
- 19 Institute of Physics, University of Stockholm, Sweden
- 20 Div. High Energy, CRN Strasbourg and Université Louis Pasteur, Strasbourg, France
- 21 Tokyo University of Agriculture and Technology and Tokyo Metropolitan University, Tokyo, Japan
- 22 Dipartimento di Fisica and INFN, Università Trieste, Trieste, Italy
- 23 Inst. für Hochenergiephysik der Osterreichischen Akademie der Wissenschaften, Vienna, Austria

**Abstract:**

Charm data from 360 GeV/c  $\pi^-p$  and 400 GeV/c  $pp$  interactions are used to give results on D-meson branching ratios. The analysis is based on 438 charm events containing 608 spatially resolved charm particle decays.

We present topological branching ratios, as well as the following inclusive branching ratios of D-mesons into kaons:

$$B(D^\pm \rightarrow K^\mp + \text{anything}) = 0.17 \pm 0.07,$$

$$B(D^\pm \rightarrow K^\pm + \text{anything}) = 0.08^{+0.06}_{-0.05},$$

$$B(D^0 \rightarrow K^\pm + \text{anything}) = 0.42 \pm 0.08,$$

$$B(D^0 \rightarrow K^+ + \text{anything}) = 0.03^{+0.05}_{-0.02},$$

and the following semielectronic branching ratios of D-mesons:

$$B(D^\pm \rightarrow e^\pm + \text{anything}) = 0.20^{+0.09}_{-0.07},$$

$$B(D^0 \rightarrow e^\pm + \text{anything}) = 0.15 \pm 0.05.$$

In this paper we report measurements of branching ratios for charm D mesons produced by  $\pi^-$ -proton interactions at 360 GeV/c and proton-proton interactions at 400 GeV/c.. These data come from experiment NA27 at the CERN SPS using the European Hybrid Spectrometer (EHS). Preliminary results on branching ratios of D mesons, based on 30% of the total statistics have already been published [1]. The results reported in this paper are final results based on the full sample of charm data obtained by the experiment. The experimental set-up has been described in detail elsewhere [2,3,4]. Briefly, it involves a large angle multiparticle spectrometer downstream of the rapid cycling LExan Bubble Chamber (LEBC) with high resolution optics [3]. The spectrometer includes the charged particle identifier ISIS [4] as well as lead-glass walls for electron and photon detection. For the proton run of the experiment it also included the Forward Čerenkov detector [3] for charged particle identification at high momenta.

The isolation of 114 events containing 183 observed charm decays from 265,000  $\pi^-$ -proton interactions seen in the bubble chamber and 324 events containing 425 observed charm decays from 1,015,000 proton-proton interactions seen in the bubble chamber has been described in detail elsewhere (see references [2] and [3] respectively). The selection procedure uses, for neutral decays with two charged tracks and charged decays with one charged decay product, a transverse momentum cut ( $p_t > 250$  MeV/c) to remove strange particle background. These two samples of decays are described as the 'full charm samples' for the pion and proton runs respectively.

### The topological branching ratios.

We first consider the topological branching ratios of neutral D mesons based on a specific subsample of the 'full charm sample' for the proton run. An unbiased sample of 2, 4 and 6 prong decays (V2, V4 and V6) is defined as all those clear (†) decays paired to a 'trigger' decay (a decay displaying explicit characteristics of charm; high multiplicity or high  $p_t$  decay products). Neutral decays in our sample were further required to be contained within a cylinder of 200 $\mu$ m radius centred on the interacting beam track. All decays passing these cuts were assumed to be  $D^0$  decays. Our sample contained 90 2-prong and 21 4-prong decays; no 6-prong decay passes our cuts. A similar analysis using the data in the 'full charm sample' for the pion run [1] yielded a sample containing 49 2-prong decays, 12 4-prong decays and no 6-prong decays. Combining these two samples and using the fraction of neutral decays extracted [5] from SPEAR results [6],

---

(†) The description 'clear' here refers to vertices not obscured (within 7 $\mu$ m) by a track from the primary interaction.

$B(D^0 \rightarrow 0 \text{ charged}) = 0.14 \pm 0.04$ , we obtain:

$$B(D^0 \rightarrow 2 \text{ charged}) = 0.69 \pm 0.04,$$

$$B(D^0 \rightarrow 4 \text{ charged}) = 0.17 \pm 0.03,$$

$$B(D^0 \rightarrow 6 \text{ charged}) < 0.01 \text{ at } 90\% \text{ C.L.}$$

In order to obtain the topological branching ratios of charged D mesons we defined an unbiased sample of 1-prong, 3-prong and 5-prong decays (C1, C3 and C5 respectively) as all those clear decays, in the 'full charm sample' for the proton run, paired to a 'trigger' decay displaying the explicit characteristics of charm. The decays in our sample were further required to be contained within a cylinder of  $600\mu\text{m}$  radius centred on the interacting beam track. Further cuts, based on the maximum impact parameter of the charged prongs from a decay (see figure 1), were applied to our sample. These cuts were designed to remove background from a short lived component ( $\Lambda_c$  baryons and F mesons) and to correct for the low detection efficiency of one-pronged decays with low impact parameters. Decays with a maximum impact parameter greater than a certain value were assumed to be  $D^\pm$  decays. Table 1 shows the number of decays in the different topologies passing our cuts, for different values of the maximum impact parameter cut. We now consider a) how to correct for the bias introduced in the sample of  $D^\pm$  decays by this cut and b) the effectiveness of the cut in removing short lived  $\Lambda_c$  baryons. The distribution of maximum impact parameters in each topology was simulated by Monte-Carlo using the experimentally determined  $x_F$  and  $p_t$  distributions of D mesons in the proton run [7], a lifetime of  $\tau = 10.7 \times 10^{-13}\text{s}$  [8] and branching ratios extracted from reference [9]. The results of the Monte-Carlo simulation were used to determine the acceptances of the different values of the maximum impact parameter cut for each topology. These acceptances which varied by  $\pm 15\%$  with topology for a given cut were then used to correct the numbers of decays passing our cut in each topology and these corrected numbers of decays were then used to obtain the topological branching ratios of charged D mesons. Table 2 shows the different values calculated for the branching ratio;  $B(D^\pm \rightarrow 1 \text{ charged})$  and for the ratio of 5-prong decays to 3-prong decays for different maximum impact parameter cuts. The distribution of maximum impact parameters for  $\Lambda_c^+$  decay in the C3 topology was simulated by Monte-Carlo assuming:  $\Lambda_c^+$  production according to  $(1 - x_F)^1$  and  $e^{-1.2p_t^2}$ , a lifetime of  $\tau = 1 \times 10^{-13}\text{s}$  and using branching ratios extracted from reference [9]. Our Monte-Carlo simulation shows that 79% of charged D meson decays compared to only 12% of  $\Lambda_c$  decays pass a  $100\mu\text{m}$  maximum impact parameter cut in the C3 topology. These acceptances are 56% and 3% respectively in the C1 topology. Furthermore, with such impact parameters the detection efficiency is high for all topologies. We therefore required the maximum

impact parameter to be greater than  $100\mu\text{m}$  in our data sample. A previous calculation [1] based on the data in the 'full charm sample' for the pion run yielded (†):

$$\frac{B(D^\pm \rightarrow C5)}{B(D^\pm \rightarrow C3)} = 0.09 \pm 0.05$$

In order to obtain final results for the topological branching ratios of charged D mesons we combined this result with the results shown in table 2 for a  $100\mu\text{m}$  impact parameter cut. Our calculation gives:

$$B(D^\pm \rightarrow 1 \text{ charged}) = 0.44 \pm 0.09$$

$$B(D^\pm \rightarrow 3 \text{ charged}) = 0.53 \pm 0.09$$

$$B(D^\pm \rightarrow 5 \text{ charged}) = 0.03 \pm 0.01$$

Where the errors quoted are statistical only. There is a further, systematic error due to uncertainty in the maximum impact parameter distributions predicted by our Monte-Carlo simulation. This is mainly due to the uncertainty in the  $D^\pm$  lifetime. We estimated these systematic errors to be negligible relative to our statistical errors. These results are now independent of the results of any other experiments.

#### The inclusive branching ratios.

To measure inclusive branching ratios to charged kaons and semileptonic channels we have defined a charm sample with additional conservative selection criteria. This, the 'fully reconstructed charm sample', is defined as all those decays in the 'full charm samples' for the pion and proton runs excluding:

- all those decays whose vertices are obscured by a track from the primary interaction (this cut excludes all unclear topologies and all cases of a charged decay which is also compatible with a neutral decay superimposed on a primary track);
- all decays with multiplicity 3 or less for which any decay track is not reconstructed in the spectrometer;
- all decays with multiplicity 4 or more for which more than one decay track is not reconstructed in the spectrometer;
- all decays with multiplicity less than 3 which were not paired to another decay displaying the explicit characteristics of charm (high multiplicity or high  $p_t$  decay products).

---

(†) Note that single prong, charged decays were ignored in this analysis since the systematic detection problems in the C1 topology were not well understood.

All tracks originating from decay vertices satisfying these cuts and possessing reliable (†) ISIS ionization information were included in our track sample. This contained a total (pion and proton runs combined) of 534 tracks from 35 1-prong, 91 2-prong, 87 3-prong, 51 4-prong, 8 5-prong and 1 6-prong decays.

Figure 2 shows the  $dE/dx$  signals for the tracks in our sample as a function of momentum. Typical error bars are also shown for three of the tracks. The measurements are seen to cluster around the expected curves for  $e, \pi, k$  and  $p$  masses. In particular a number of clearly separated electrons are seen. In many cases the  $\chi^2$  probabilities for different mass assignments to the decay tracks permit unique identification at the 1% level. Nevertheless, we have used a maximum likelihood analysis to achieve bias free estimates with the smallest errors, of the proportions of different masses in the decay prong sample. The likelihood function,  $L$ , of the number,  $n_\alpha$ , of particles of each mass,  $\alpha$ , is given by [10,11]:

$$\ln L(n_\alpha) = \sum_j \left[ \ln \left[ \frac{1}{s} \times \sum_\alpha n_\alpha e^{-0.5 \times \left( \frac{Z_{oj} - Z_{\alpha j}}{\sigma_j} \right)^2} \right] \right] - \sum_\alpha n_\alpha$$

Where  $Z_{oj}$  is the logarithm of the measured ionization for the  $j^{\text{th}}$  track,  $Z_{\alpha j}$  is the logarithm of the expected ionization of this track if it were an electron, pion, etc... and  $\sigma_j$  is the resolution of the logarithm of the ionization. The latter is given by  $\sigma_j = s/\sqrt{N_j}$ , where  $s$  is a resolution parameter and  $N_j$  is the number of ionization measurements in ISIS [4]. The value of the resolution parameter,  $s$ , was determined for the pion and proton data separately by plotting the maximum value of  $\ln L(n_\alpha)$  against  $s$  for 937 tracks with reliable ISIS ionization information from the events in the 'full charm sample' for the pion run and 2245 tracks with reliable ISIS ionization information from the events in the 'full charm sample' for the proton run. For the pion data, the result was  $s = 0.57 \pm 0.02$ , consistent with the known value of 0.56, previously obtained from an analysis of strange particle decays [4]. The result was  $s = 0.62 \pm 0.02$  for the proton run data. The search for the maximum likelihood solution was found to converge rather rapidly. For non-zero values of  $n_\alpha$ , one standard deviation errors were taken from the values at which  $\ln L$  dropped by 0.5 from its peak value (maximizing with respect to other  $n$ ). In appropriate cases the 90% confidence level upper

---

(†) We excluded from our sample those tracks falling in the 'beam region' of ISIS [4] where there is a pronounced localised loss of gas amplification due to local space charge. Unresolved double tracks giving ionization values in the range  $I/I_0 = 2.0$  to 3.2 were also excluded from our sample. We further required the distribution of pulse heights along each track to be consistent with uniformity at the 4 s.d. level which removes residual cases of partially overlapping tracks.

or lower limits were also calculated from a normalised plot of the likelihood function against  $n_\alpha$ . These errors describe the combined effect of uncertainties in particle identification and statistical fluctuations in the sample [11].

There is no significant evidence for muons in the 'full charm samples' for the pion and proton runs. The likelihood method prefers 37 muons (compared with  $56_{-9}^{+10}$  electrons in the same sample) but, because the muons and pions are barely separated, the 90% confidence level upper limit is more than 120 muons. Removal of the muon hypotheses does not make any difference to the numbers of electrons, protons and kaons or their errors as given by the maximum likelihood. Therefore in the following we ignore muons.

The number of protons, kaons and electrons in the neutral and charged decay topologies are shown in table 3. There is no evidence in our data for a neutral charm baryon. The figures given in brackets in table 3 correspond to 90% confidence level upper limits. We estimate a 90% confidence level upper limit of  $0.2\mu\text{b}$  for the production cross-section of such a state with Feynman- $x$  greater than zero decaying inclusively to a proton (assuming a lifetime greater than  $2 \times 10^{-13}\text{s}$ ). The figure for the proton content of the charged decay track sample shows evidence for positively charged charm baryons decaying inclusively to protons (or charge conjugates). In order to remove this charm baryon background from our sample we used a  $100\mu\text{m}$  maximum impact parameter cut for our charged decays (as described in our topological branching ratio analysis). Table 4 shows the numbers of protons, kaons and electrons in the different decay topologies as given by the maximum likelihood analysis after the maximum impact parameter cut was applied. Using our Monte-Carlo simulated distribution of maximum impact parameters for  $\Lambda_c^+$  decays we estimate that a background of  $1.6_{-0.8}^{+1.1}$  charm baryon decays remain in our sample of 89 charged D meson decays (assuming inclusive branching ratios to protons of order 0.4).

To transform the numbers of table 4 into inclusive branching ratios for the decays  $D^\pm \rightarrow K^\mp + X$ ,  $D^\pm \rightarrow K^\pm + X$  and  $D^0 \rightarrow K^\pm + X$  we correct for the small bias due to the geometrical acceptance of ISIS. This was estimated by Monte-Carlo simulation using the observed  $x_F$  and  $p_t$  dependences for D mesons [2,7]. There is a further systematic effect which can give rise to a small bias in the figures of table 4; of the tracks within the acceptance of the ISIS fiducial volume the high momentum ones are more likely to lose their  $dE/dx$  measurements because of track overlap or the limited storage capacity of ISIS for  $dE/dx$  measurements. Such high momentum tracks are enriched in kaons and protons. This systematic effect was more significant in the proton run of the experiment; for which the charged particle flux in the ISIS fiducial volume was higher. This



from 11 V4 decays and 35 V2 decays. An analysis analogous to the one previously described yielded a result of  $B(D^0 \rightarrow K^\pm + X) = 0.41_{-0.12}^{+0.14}$ , which is clearly compatible with the value reported above. The result obtained for the inclusive branching ratio for the decay  $D^0 \rightarrow K^+ + X$  was:

$$B(D^0 \rightarrow K^+ + X) = 0.03_{-0.02}^{+0.05}$$

To be compared with a previous world average of  $0.08 \pm 0.03$  [9].

### The semielectronic branching ratios

The electron content for each topology is shown in table 4. Using our Monte-Carlo simulation of the acceptance bias of ISIS we find that the number of electrons observed is expected to be underestimated by 5% in the C1 topology, 4% in the C3 and C5 topologies and 6% in the V2 and V4 topologies. These 'acceptances' biases already combine the effect of the limited geometrical acceptance of ISIS and the effect of the loss of ionization measurements through track overlap or limited storage capacity. There is an underestimate of 4% in all topologies due to the difference between the interaction length (1%) and the radiation length (5%) between the bubble chamber and the centre of ISIS. In the C1 topology there is a further 1% overestimate due to the fact that decays with light charged particles in the final state are more likely to pass our maximum impact parameter cut. This effect was estimated to be negligible ( $< 0.5\%$ ) in the C3 and C5 topologies.

The figures for the electron content in table 4 were corrected for these small (relative to our statistical errors) biases and combining with the topological branching ratios we obtain:

$$B(D^\pm \rightarrow e^\pm + X) = 0.20_{-0.07}^{+0.09},$$

$$B(D^0 \rightarrow e^\pm + X) = 0.15 \pm 0.05.$$

While our result for the semielectronic branching ratio of charged D mesons is clearly compatible with the result reported by Baltrusaitis et al. [12],  $B(D^\pm \rightarrow e^\pm + X) = 0.170 \pm 0.019 \pm 0.007$ , our result for neutral D mesons is incompatible with the result reported by them,  $B(D^0 \rightarrow e^\pm + X) = 0.075 \pm 0.011 \pm 0.004$ . Their value would lead us to expect 9 electrons in our sample of tracks from neutral D meson decays. We have observed more than 13; a result with a probability less than 8%, calculated on Poisson statistics.

We consider our total data sample more closely. The likelihood function for the number of electrons in the V2 decay prong sample is shown in figure 3. Including the event in V4 with an electron identified by the lead-glass detectors [1], the 90% confidence level lower limit for the semielectronic branching ratio of neutral D mesons is 0.10, corresponding to the observation of 8.7

effect was simulated in our Monte-Carlo by using observed distributions of the number of  $dE/dx$  measurements per track. From this Monte-Carlo simulation we estimate that the number of kaons observed is too great by 9% in the V2 and V4 topologies and 10%, 10% and 11% in the C1, C3 and C5 topologies respectively. There is a further correction in the charged decay topologies due to a small decay mode dependence of the proportion of D meson decays passing our maximum impact parameter cut. The magnitude of this correction was calculated using the Monte-Carlo simulated maximum impact parameter distributions. We estimate this bias to be negligible (*i.e.*  $< 0.5\%$ ) in the C3 and C5 topologies but in the C1 topology this leads to an underestimate of 7% in the number of kaons.

Applying these corrections to the numbers in table 4 we find the following ratios:

$$D^{\pm} \rightarrow K^{\mp} \text{ in C3/all C3} = 0.33^{+0.13}_{-0.11},$$

$$D^{\circ} \rightarrow K^{\pm} \text{ in V2/all V2} = 0.47^{+0.10}_{-0.09},$$

$$D^{\circ} \rightarrow K^{\pm} \text{ in V4/all V4} = 0.58 \pm 0.18,$$

$$D^{\pm} \rightarrow K^{\pm} \text{ in C1/all C1} = 0.19^{+0.12}_{-0.10},$$

$$D^{\pm} \rightarrow K^{\pm} \text{ in C3/all C3} < 0.08 \text{ at } 90\% \text{ C.L.},$$

and combining with the topological branching ratios given earlier:

$$B(D^{\pm} \rightarrow K^{\mp} + X) = 0.17 \pm 0.07,$$

$$B(D^{\circ} \rightarrow K^{\pm} + X) = 0.42 \pm 0.08,$$

$$B(D^{\pm} \rightarrow K^{\pm} + X) = 0.08^{+0.06}_{-0.05}.$$

We note that the  $D^{\pm}$  results refer to decay kaons of specified charge whereas the  $D^{\circ}$  result refers to  $K^{\pm}$  regardless of charge. These results compare with previous world averages of  $0.16 \pm 0.04$ ,  $0.52 \pm 0.10$  and  $0.060 \pm 0.033$  respectively [9].

In order to obtain separate inclusive branching ratios for the decays  $D^{\circ} \rightarrow K^{+} + X$  and  $D^{\circ} \rightarrow K^{-} + X$  we selected a sample of neutral decays of known charm. Our sample was defined as all those clear, neutral decays in the 'full charm samples' displaying the explicit characteristics of charm (high multiplicity or high  $p_t$  decay products) and paired to another charm decay candidate in the same event. We restricted our analysis to those neutral decays whose charm signature was known either because they were paired to a clear, charged charm decay candidate of unambiguous charge or because they were paired to a charm decay candidate with an electron identified in the spectrometer (†). Our sample contained a total of 75 tracks with reliable ISIS ionization information

(†) Identified by the lead-glass detectors or uniquely identified at the 1% level from the ISIS ionization measurement.

decay of a charm particle if one of the tracks of the electron-positron pair is not identified in the spectrometer. We expect a background of 1.6 Dalitz conversions in our neutral D meson sample, mainly in the high multiplicity topologies (*i.e.* V4 and V6). In fact two V4 decays and one V6 decay have been identified as Dalitz events and removed from our sample. The remaining semileptonic V4 contains an electron identified by the lead-glass detectors [1] and is not compatible with a Dalitz event. It is therefore treated as a signal. In the charged D meson decay sample, the background expected from asymmetric Dalitz pairs is less than 0.9 events. Furthermore, this background is charge symmetric and there is no evidence in the figures in table 4 for 'wrong sign' electrons of the type  $D^\pm \rightarrow e^\mp + X$ .

The semielectronic branching ratios we have obtained may be combined with previous NA27 results on D meson lifetimes [8],

$$\begin{aligned}\tau(D^\pm) &= 11.2_{-1.1}^{+1.4} \ 10^{-13}\text{s}, \\ \tau(D^0) &= 4.6_{-0.8}^{+0.6} \ 10^{-13}\text{s},\end{aligned}$$

to give results on partial widths:

$$\begin{aligned}\Gamma(D^\pm \rightarrow e^\pm \text{ inclusive}) &= 18_{-7}^{+8} \ 10^{10}\text{s}^{-1}, \\ \Gamma(D^0 \rightarrow e^\pm \text{ inclusive}) &= 33_{-12}^{+11} \ 10^{10}\text{s}^{-1}.\end{aligned}$$

Since there are no simple, first order diagrams which are different for  $D^0$  and  $D^\pm$  semileptonic decay, we expect  $\Gamma(D^0 \rightarrow e^\pm \text{ inclusive})$  to be equal to  $\Gamma(D^\pm \rightarrow e^\pm \text{ inclusive})$ .

In conclusion, we have reported results on  $D^0/\bar{D}^0$  and  $D^\pm$  topological branching ratios and inclusive charged kaon and semielectronic branching ratios. The results are based on modest statistics but have negligible systematic errors.

electrons in the V2 track sample. That the electron content of our neutral decay prong sample is not reliant on the likelihood analysis used was shown in our previous paper [1]. Monte-Carlo simulation has shown that out of 12.7 electrons in our V2 track sample, 4.0 are expected to reach the geometrical acceptance of the gamma detectors. In fact our V2 track sample contains 3 tracks which are labelled as electrons by the gamma detectors.

There was no evidence in our sample of neutral decays of known charm signature for 'wrong sign' electrons of the type  $D^0 \rightarrow e^- + X$ ; the 90% confidence level upper limit for the branching ratio was  $B(D^0 \rightarrow e^- + X) < 0.09$ .

We have carried out checks on the particle identification. First, the ISIS signals of 273 tracks labelled as hadrons and 15 tracks labelled as electrons by the gamma detectors were analysed separately using the maximum likelihood method. These were all the tracks identified by the gamma detectors, which originated from decays contained in the events of the 'full charm samples' and which possessed reliable ISIS ionization information. The results of the likelihood analyses are shown in table 5. The most likely number of electrons in our sample of gamma detector hadrons was zero; also there was no significant evidence for any hadrons in our sample of gamma detectors electrons. Secondly, the particle composition of four samples of tracks vetoed as electrons, pions, kaons or protons by the Forward Čerenkov detector, was determined using the maximum likelihood technique on ISIS ionization information. These samples were extracted from all the tracks in the events of the 'full charm sample' for the proton run with particle identification by the Forward Čerenkov detector and reliable ISIS ionization information. The results of the likelihood fits are shown in table 6. We conclude that there is strong evidence that neither ISIS nor the analysis procedure has misidentified hadrons as electrons.

Finally, we consider the background when tracks are genuine electrons. Any electron-positron pair from  $\gamma$ -conversion in the charm box could be misinterpreted as semileptonic through wrong reconstruction in the spectrometer. In general such a candidate would appear as an unpaired V2 semileptonic decay. A maximum likelihood fit to the prongs of all V2 decays which survived our selection procedure but did not have a charm pair yields a 90% confidence level upper limit of 9.5 semileptonic decays. The probability of a background event in paired V2 is therefore less than 0.35%. The same argument applies to the background from genuine semileptonic decay of strange particles. A similar calculation for the sample of C1 decay prongs yields an upper limit for the probability of having a strange semileptonic C1 in the paired decay sample of 0.30%.

Another possible source of background are Dalitz conversions of neutral pions produced in the

## References

- [1] LEBC-EHS Collab., M. Aguilar-Benitez et al., *Phys. Lett.* **168B** (1986) 170.
- [2] LEBC-EHS Collab., M. Aguilar-Benitez et al., *Z. Phys.* **C31** (1986) 491.
- [3] LEBC-EHS Collab., M. Aguilar-Benitez et al., 'The European Hybrid Spectrometer', CERN/EP 87-31  
(submitted to *Nucl. Inst. and Meth.*)
- [4] W.W.M. Allison et al., *Nucl. Inst. and Meth.* **224** (1984) 396.
- [5] LEBC-EHS Collab., M. Aguilar-Benitez et al., *Phys. Lett.* **135B** (1984) 237.
- [6] I. Peruzzi et al., *Phys. Rev. Lett.* **39** (1977) 1301,  
R.H. Schindler et al., *Phys. Rev. D* **24** (1981) 78,  
G.H. Trilling, *Phys. Rep.* **75** (1981) 57.
- [7] LEBC-EHS Collab., M. Aguilar-Benitez et al., 'D meson production from 400 GeV/c  $pp$  interactions', CERN/EP 87-45  
(submitted to *Phys. Lett. B*).
- [8] LEBC-EHS Collab., M. Aguilar-Benitez et al., 'D meson lifetimes', CERN/EP 87-38  
(submitted to *Phys. Lett. B*).
- [9] M. Aguilar-Benitez et al., *Phys. Lett.* **170B** (1986).
- [10] J. Orear, UCRL-8417, 1958 (unpublished).
- [11] L. Lyons, W.W.M. Allison & J. Pañella Comellas, *Nucl. Instr. and Meth.* **A245** (1986) 530.
- [12] R.M. Baltrusaitis et al., *Phys. Rev. Lett.* **54** (1985) 1976.

Table 1

Topology	Number of decays with maximum impact parameter greater than			
	7	80	100	120
C1	51	35	32	29
C3	66	61	56	53
C5	3	3	3	3

Table 2

	Maximum impact parameter greater than ( $\mu m$ )			
	7	80	100	120
$B.R.(D^{\pm} \rightarrow C1)$	$0.43 \pm 0.07$	$0.43 \pm 0.08$	$0.44 \pm 0.09$	$0.44 \pm 0.09$
$\frac{B.R.(D^{\pm} \rightarrow C5)}{B.R.(D^{\pm} \rightarrow C3)}$	$0.045 \pm 0.027$	$0.045 \pm 0.027$	$0.049 \pm 0.029$	$0.051 \pm 0.030$

Table 3.

We label the decays C<sub>n</sub> and V<sub>n</sub>; these stand for decays of charged and neutral particles with n charged decay products respectively. For decays of charged particles the 'likesign' sample contains the decay tracks with the same charge as the parent particle and the 'unlikesign' sample the decay tracks with charge of opposite sign to that of the parent particle. The figures shown in brackets correspond to 90% confidence levels and blank entries (-) imply that the value preferred by the likelihood function is zero.

Topology of vertices	Number of decay vertices	Fraction tracks with ionization information	Most likely number of:		
			protons	kaons	electrons
V2	84		(< 10.1)		
V4	51	278/378	-	57.5 <sup>+9.6</sup> <sub>-9.6</sub>	14.1 <sup>+6.1</sup> <sub>-4.3</sub>
V6	1				
		Likesign			
C1	36	178/234	5.8 <sup>+4.1</sup> <sub>-3.0</sub>	7.5 <sup>+6.5</sup> <sub>-4.1</sub>	19.3 <sup>+6.2</sup> <sub>-5.3</sub>
C3	87				
		Unlikesign			
C5	8	60/103	(< 7.4) 1.9(†)	19.2 <sup>+5.8</sup> <sub>-5.1</sub>	(< 2.8) -

(†) The likelihood function prefers this result rather than zero with a likelihood ratio of 12 to 1.

Table 4

Topology of vertices	Number of decay vertices	Fraction tracks with ionisation information	Most likely number of:		
			protons	kaons	electrons
C1	23	23/23	(< 5.3) -	4.4 <sup>+3.0</sup> <sub>-2.3</sub>	5.8 <sup>+3.1</sup> <sub>-2.6</sub>
V2	84	134/168	(< 5.3) -	34.1 <sup>+7.3</sup> <sub>-6.8</sub>	12.7 <sup>+4.7</sup> <sub>-3.9</sub>
C3	60	Likesign 85/120	(< 3.0) -	(< 3.7) -	4.9 <sup>+3.6</sup> <sub>-2.4</sub>
		Unlikesign 34/60	(< 3.3) -	12.3 <sup>+4.6</sup> <sub>-4.3</sub>	(< 2.7) -
V4	51	140/204	(< 8.9) -	22.3 <sup>+6.9</sup> <sub>-7.0</sub>	(< 4.9) 1.0 (†)
C5	7	Likesign 13/21	(< 2.1) -	(< 2.6) -	(< 2.7) -
		Unlikesign 6/14	(< 4.0) 1.0 (‡)	(< 3.4) -	(< 3.1) -
V6	1	4	(< 2.5) -	(< 4.4) -	(< 1.9) -

(†) There is one electron identified by the lead-glass detectors and supported but not required by ionisation [1]. This has been inserted by hand.

(‡) The likelihood function prefers this result rather than zero with a likelihood ratio of 1.9 to 1.



**Table 5**  
**ISIS-Gamma Detector comparison**

Gamma detector information	Number of tracks	Most likely (ISIS info.) number of:			
		Electrons	Pions	Kaons	Protons
Hadrons	273	0.0	228.6	40.8	3.6
Electrons	15	14.3	0.7	0.0	0.0

**Table 6**  
**ISIS-Forward Čerenkov comparison**

Forward Čerenkov vetoed	Number of tracks	Most likely (ISIS info.) number of:			
		Electrons	Pions	Kaons	Protons
Electrons	29	0.2	7.7	21.1	0.0
Pions	17	0.0	0.0	17.0	0.0
Kaons	85	0.0	82.9	2.1	0.0
Protons	101	0.0	99.8	1.2	0.0

## Figure captions

### Figure 1

The impact parameter  $y$ , defined in the film plane projection with unit magnification to the chamber. The impact parameter shown corresponds to track 3. In the decay illustrated it is track 1 which has the largest impact parameter and it is to this which we refer to as the maximum impact parameter of the decay.

### Figure 2

ISIS  $dE/dx$  signals as a function of momentum for the charm decay tracks from the 'fully reconstructed charm sample' discussed in the text. The curves show the expected behaviour for electrons, pions, kaons and protons. Typical errors are shown. Circles are the  $dE/dx$  signals of the only tracks found to be associated with electromagnetic showers of the correct energy (to within 20%) in the lead-glass detectors.

### Figure 3

Likelihood function versus the number of electrons in the V2 sample for the pion and proton runs combined. The shaded area represents the region excluded at the 90% confidence level. The corresponding values of the semielectronic branching ratio are also shown.

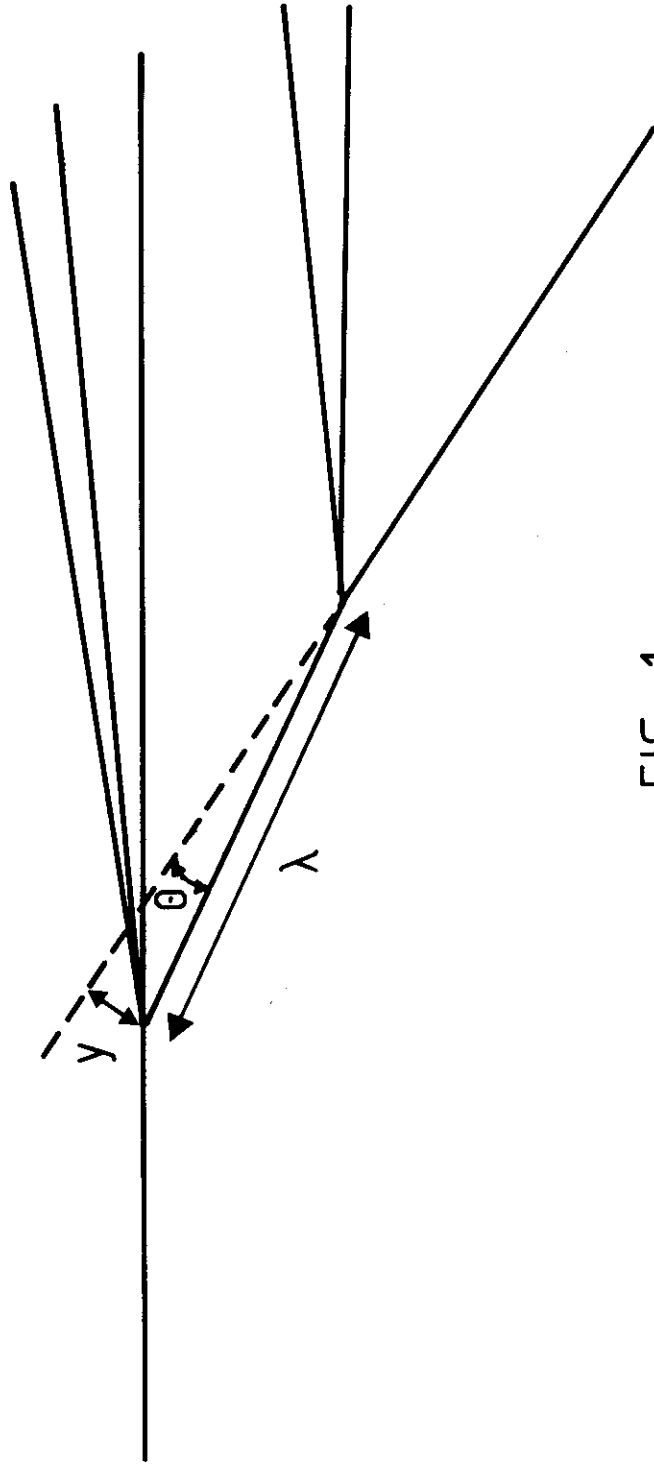


FIG. 1

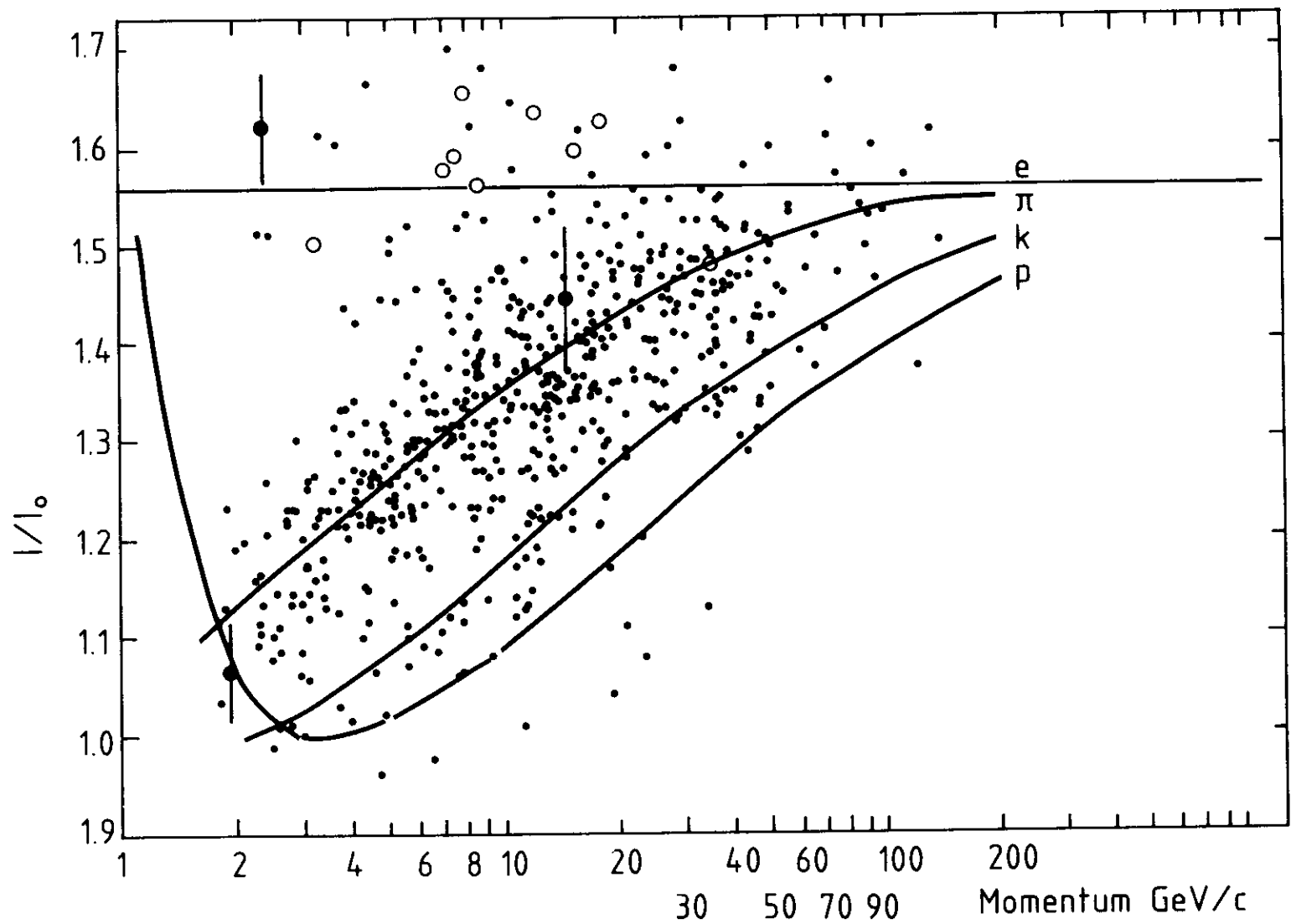


FIG. 2

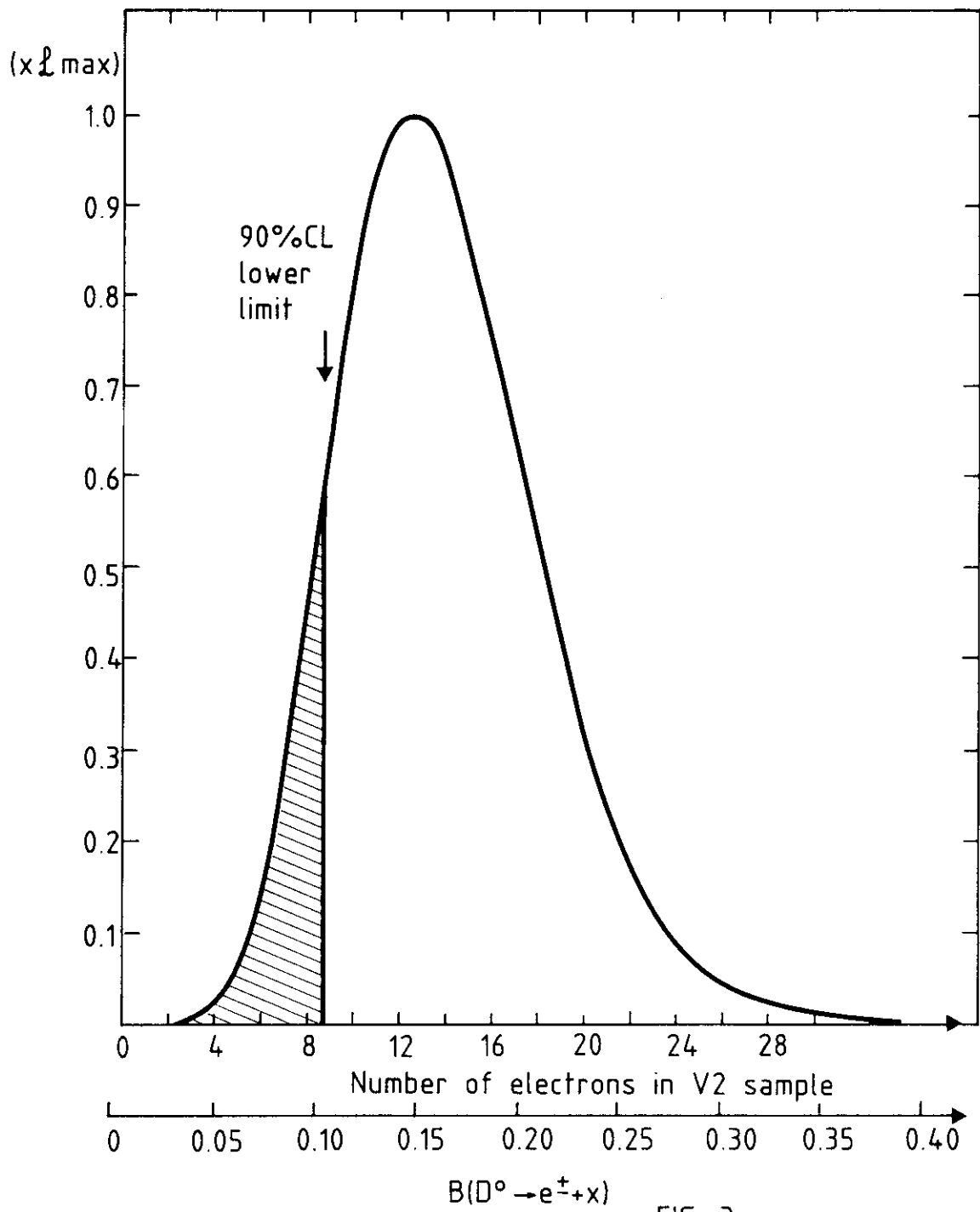


FIG. 3